Farmland Fertility Optimization with Deep Learning based COVID-19 Detection for Healthcare Decision Making

Ahmed Hatip[*1], Necati Olgun [2], Sandy Montajab Hazzouri [3]

[1] Gaziantep University, Department of Mathematics, Gaziantep, Turkey
[2] Gaziantep University, Department of Mathematics, Gaziantep, Turkey
[3] Faculty of Informatics Engineering , Albaath University, Syria
Emails: kollnaar5@gmail.com; olgun@gantep.edu.tr; Samonhaco1994@gmail.com

Abstract

Machine Learning (ML) and Artificial Intelligence (AI) are being employed in the fight against COVID19 by supporting the analysis of medical images, like X-rays and CT scans, to find characteristic paradigms linked with the virus. AI methods can evaluate huge volumes of data, which includes imaging data and patient medical records, for enriching the speed and precision of COVID19 diagnosis. Also, the use of ML and AI in medical imaging can aid in detecting new variants of viruses and forecasting their spread. The integration of ML and AI in COVID19 healthcare has greater potential to enhance the efficiency and accuracy of diagnoses along with that informing public health decision-making. Thus, the study proposes a Farmland Fertility Optimization Algorithm with Deep Learning based Healthcare Decision Making (FFOADL-HDM) approach for the detection of COVID19. The presented FFOADL-HDM approach emphasises the identification and classification of COVID19 using a CT scan. To achieve this, the FFOADL-HDM method exploits a modified SqueezeNet model for the generation of feature vector. Also, the hyperparameters of the modified SqueezeNet model can be selected by the use of FFOA. At last, the COVID-19 detection procedure is executed by the use of Adamax optimizer with (CFNN). The stimulation analysis of the FFOADL-HDM algorithm is studied on the SARS-CoV-2 CT image dataset from the Kaggle repository. The results highlighted the improved detection rate of the FFOADL-HDM technique over recent state of art approaches

Keywords: Artificial Intelligence; COVID19 diagnoses; Computed tomography scans; Machine learning; Healthcare; Decision making

1. Introduction

COVID-19 or coronavirus disease become a global pandemic, which had greater impacts on all walks of human life [1]. At an initial stage, diagnosing COVID19 is indispensable to decreasing the mortality rate. In this article, a cascaded system was developed for segmenting the lung, quantifying, detecting, and localising, COVID19 infections from computed tomography (CT) images. COVID19 can be confirmed by the nucleic acid amplification test of blood samples or respiratory tract by leveraging reverse transcription-polymerase chain reaction (RT-PCR) [2]. But its sensitivity was limited, and the outcome was deeply operator dependent. Above all, it consumes more time, which can be a main challenge as novel variants of COVID19 spread fast. So, finding replacements for the RT-PCR test is vital [3]. Automatic analysis of medical images, like CT and CXR scans, is employed as an alternative, since the analysis takes lesser period and can be very stable likened to the RT-PCR test. Even images were less dependent and more dependable on operators [4]. As well, numerous works show that COVID19 has a harmful and significant effect on the lungs, even in the primary stage of the disease, which are detected by CT images. Similarly, a lot of inspections have revealed that along with medical clinical symptoms [5], both testing and biochemical blood and lung CT images were valuable diagnosis tool to determine the conditions.

Radiotherapists are needed to analyse the CT images. In this pandemic period, a greater number of radiologists are demanded to diagnose COVID19. But it is a time error-prone and consuming task [6]. Thus, the automatic

Doi: https://doi.org/10.54216/IJAACI.050103
Received: June 17, 2023 Revised: November 11, 2023 Accepted: December 19, 2023

identification of COVID19 from chest images was needed. Deep learning (DL) methods were broadly employed in the automated analysis of radiological images [7]. It was found that DL methods were utilized for Tuberculosis screening in chest X-rays. Such techniques are capable of training weights of networks on large data along with that fine-tuning weights of pretrained networks on smaller datasets [8]. Developing artificial intelligence (AI)-related solutions specific to severity quantification and identification of COVID19 can provide an efficient, fast, and reliable substitute that can supplement orthodox medical diagnosis methods [9]. Current studies exhibited that existing deep convolutional neural network (DCNN) can exceed or reach the performance of healthcare specialists in many medical image diagnosis tasks like lung pathology screening, skin lesion classification, breast cancer detection, and brain tumor detection [10].

This study projects a Farmland Fertility Optimization Algorithm with Deep Learning based Healthcare Decision Making (FFOADL-HDM) approach for COVID19 detection. The proposed FFOADL-HDM technique emphasises the identification and classification of COVID19 using a CT scan. To achieve this, the FFOADL-HDM method exploits a modified SqueezeNet method for feature vector generation. As well, the hyperparameters of the modified SqueezeNet model can be selected by the use of FFOA. At last, the COVID19 detection procedure can be carried out by the use of an Adamax optimizer with a cascade forward neural network (CFNN). The result analysis of the FFOADL-HDM approach is studied on the SARS-CoV-2 CT scan image dataset from the Kaggle repository.

2. Related Works

Hasoon et al. [11] developed an innovative technology for earlier diagnosis and classification of COVID19 with image processing through X-ray images. A series of procedures were implemented, which includes preprocessing (morphological operation, removal of image noise, and image thresholding), ROI segmentation detection and, feature extraction, Haralick texture features, LBP, and HOG and classification (KNN) and SVM). Shahin et al. [12] intend to classify and detect coronavirus with the use of ML. To identify and spot coronavirus in CT-Lung screening a system called Computer-Assisted diagnoses (CAD) was devised for classifying and distinguishing COVID19. By using the medical specimens gained from the corona-infected patients with ML approaches like DT, SVM, Radial Basis Function, and K-means clustering.

The authors [13] modelled a novel structure for lung disease prediction such as Covid19 and pneumonia from chest images of patients. This structure has accurate estimation of region of interest (ROI), dataset acquisition, disease anticipation, image quality enhancement, feature extraction. Soft computing techniques such as SVM DL, ANN, KNN, and ensemble classifiers were employed for classification. In [14], DL-related methods particularly deep extraction of features, finetuning of pretrained CNN, and end-to-end training were leveraged for distinguishing normal (healthy) and COVID19 chest X-ray imageries. Ahemad et al. [15] end goal of this study was to implement ML for classifying and identifying coronaviruses. COVID-19 was expected to be categorized and discriminated against in CAD and CT-Lung screening. Various ML approaches, which include DT, SVM, Radial Basis Function, and K-means clustering, are used with medical samples from patients who are infected by corona.

Katsamenis et al. [16] developed a DL structure that classifies COVID19 pneumonia in thoracic radiographs, along with that distinguishes it from bacterial pneumonia infection. Deep classifier methods, like CNNs, need large-scale data that should be performed and trained properly. TL appear as the go-to technique for alleviating the demand for trained data, as the number of X-ray samples relevant to COVID19 is restricted and developed precise automatic diagnosis methods. Le et al. [17] presented an innovative IoT-empowered Depthwise separable CNN (DWS-CNN) with Deep SVM (DSVM) for COVID19 classification and diagnosis. Firstly, data of patients will be gathered in the data acquisition phase with the use of IoT gadgets and transferred to a cloud server. After that, the DWS-CNN algorithm was employed to replace default convolution for the automatic extraction of features. Lastly, to regulate binary and multiple classes of COVID19, the DSVM method was implemented.

3. Materials and Methods

In this study, we have established a new FFOADL-HDM method for the COVID19 recognition process. The proposed FFOADL-HDM technique mainly concentrated on the development of the COVID-19 classification model using CT images. It encompasses a modified SqueezeNet feature extractor, FFOA-based hyperparameter tuning, CFNN-based classification, and Adamax optimizer-based parameter optimization. Fig. 1 demonstrates the working flow of FFOADL-HDM method.

Doi: https://doi.org/10.54216/IJAACI.050103
Received: June 17, 2023 Revised: November 11, 2023 Accepted: December 19, 2023

A. Data Used

The SARS-CoV-2 CT scan database accessible on Kaggle [18] was utilized for experimental purposes. The database contains an entire of 2492 CT scans among them 1230 are negative for SARS-CoV-2 infection viz. COVID19 (-ve) and the rest 1262 are positive for SARS-CoV-2 infection viz. COVID19 (+ve).

B. Feature Extraction: Modified SqueezeNet

The modified SqueezeNet model is used to produce a group of feature vectors. The typical CNN comprises one fully connected layer, two max-pooling layers, three convolutional layers, and an input layer [19]. The input layer gets the image where the pixel contributed towards the resultant via a series of kernel filters, called masks or weights. Generally, the filter used was fixed, based on the network layer, the output being the results of 2D convolution operation:

$$U = conv2d\,(X, W) \tag{1}$$

In Eq. (1), X and U are the input and output images, and W indicates the 2D filter matrix or weight matrix.

Also, a nonlinear function σ was included in the linear part of the U layer, where the output is attained:

$$z_{mn} = \sigma(u_{mn} + b), or\ Z = \sigma(W * X + B) \tag{2}$$

Where σ signifies the sigmoid activation function, B characterizes bias for the layer, and Z denotes a mapping feature.

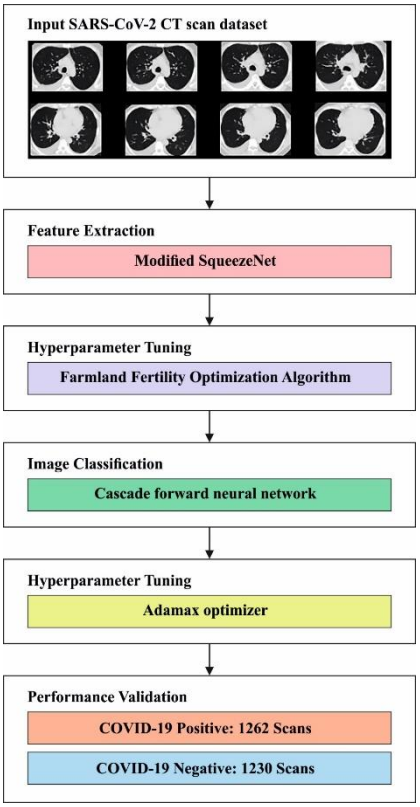

Figure 1: Workflow of FFOADL-HDM approach

For the provided 2D image (I), the convolution of mapping feature (X) through weight matrices (W) in a provided point ($I(p, q)$) as shown below:

$$\mathrm{U_{p,q}} = (\mathrm{W} * \mathrm{X})_{\mathrm{p,q}} = \sum_{m=0}^{r-1} \sum_{n=0}^{c-1} \mathrm{W_{m,n} X_{p-m,q-n}} \tag{3}$$

SqueezeNet comprises network-designed architecture 50 times smaller than AlexNet. Due to its fast execution and performance, the SqueezeNet model is widely applied in the healthcare field.

Doi: https://doi.org/10.54216/IJAACI.050103
Received: June 17, 2023 Revised: November 11, 2023 Accepted: December 19, 2023

Followed by the eight fire modules, a SqueezeNet model is made up of standalone convolution layer, accountable to receive the input images, and ends up having a convolution layer. The network can be represented as a sequence of "squeeze", encompassed by 1x1 filters, and "expand", encompassed by a sequence of 1x1 and 3x3 filter, layers. The combination of these two layers was called a Fire module. Fig. 2 shows the architecture of the modified SqueezeNet. During the test application of a SqueezeNet, it has been noted that the architecture outperforms other models; but the resulting metrics offered lesser value than others. A set of trials has been implemented to change the original SqueezeNet model which aims to increase the network performance. Consequently, the presented model encompassed 7 Fire modules, 1 input layer, 6 pooling layers having a pooling size of 2x2, 1 global pooling layer, 1 full connection layer, and 1 batch normalization layer was produced.

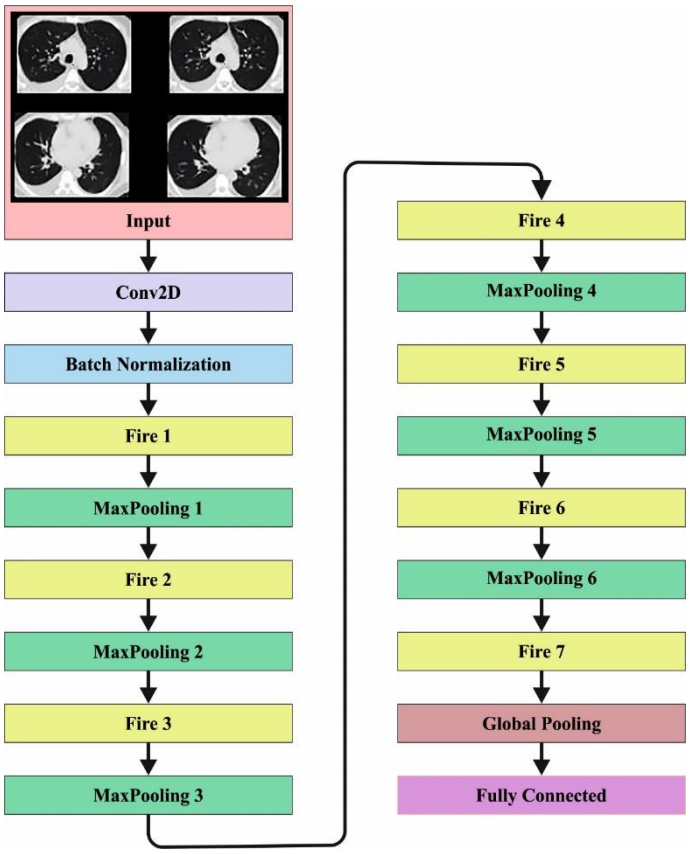

Figure 2: Structure of modified SqueezeNet

C. Hyperparameter Tuning: FFOA

At this phase, the FFOA selects the hyperparameter linked to the SqueezeNet technique. The FFOA system solves the optimizing issue by simulating the farmer performances however implementing several fertilizers for farmland with varied quality of soils [20]. During this approach, the fertilization approach to the land was equal to individuals, and the quality of soils have capable of the fitness value of individuals. To land with bad-quality soils, a better fertilizer plan has been selected; for another land, the fertilization design has been arbitrarily selective. The soil quality of farmlands is efficiently improved with the continuous development of the fertilization approach.

The pseudocode of FFOA is displayed in Algorithm 1. Essential stages can be detailed described under. It could be regarded that the count of individuals is N, and every individual X_i can be illustrated as $X_i = [X_{i1}, X_{i2}, X_{i3}, \dots, X_{iD}](i = 1,2, \dots, N)$, whereas D implies the dimension of optimizer issue, $X_{ij}(j = 1,2, \dots, D)$ signifies the value of i^{th} individuals in the j^{th} dimensional, and N signifies the individuals can be arbitrarily produced employed as:

$$X_{ij} = L_j + rand \times (U_j - L_j) \quad (4)$$

whereas Uj and Lj signify the upper and lower bounds of searching ranges, correspondingly. $rand$ refers to the arbitrary value within [0,1]. This approach of separating the farmland field is as follows. Initially, the individuals can be numbered. Next, dependent upon the primary individuals, n sequential individuals can be divided as one

Doi: https://doi.org/10.54216/IJAACI.050103
Received: June 17, 2023 Revised: November 11, 2023 Accepted: December 19, 2023

area but it could be similarly divided as k regions. The value of k has an integer superior to 2 and lower than 4; when no special criteria were offered, if $k = 4$, this approach reached the best efficacy.

An individual contained in every region is illustrated as:

$$s_a = \{x_{(a-1)\times n+1}, x_{(a-1)\times n+2}, \dots, x_{(a-1)\times n+n}\}, (a = 1,2, \dots, k) \quad (5)$$

whereas stands for subregion number, i.e., $a \in [1, k]$, and $a \in N^+; n = N/k$; and S_a indicates the set of individuals contained in the region a. For minimizing issues, the region with bad average soil S_{worst} defines the region that is maximal average fitness value of the individual. A specific computation was represented as:

$$S_{worst} = \arg\max \left\{ Fit_a = \frac{\sum_{i=1}^{n} f\,it(S_a(i))}{n} \right\} \quad (6)$$

In which fit$(S_a(i))$ denotes the value of fitness of i^{th} individuals from field a.

The memory contains local as well as global memory. An initial M_L individual having greater quality of soils in every area has been stored from local memory, however, the initial M_G individuals having greater quality soils in the complete field can be saved in the global memory. M_L and M_G demonstrate the employing the subsequent equations:

$$M_L = round(t \times n) \quad (7)$$

$$M_G = round(t \times N) \quad (8)$$

whereas t implies randomly generated value among [0.1,1] $round$ defines rounding outcomes.

The soil optimizing contains two systems the development of individuals from the sub-region with worse quality soils and the progress of individual in the other subregions. A specific optimized system is given below. To enrich the quality of soils of the poor field as possible, an individual within it employs the most effectual fertilization methods to create novel individuals illustrated as:

$$X_{inew} = h_1 \times (X_i - X_{MGlobal}) + X_i, (i = 1,2, \dots, n) \quad (9)$$

whereas $X_{MGlobal}$ denotes arbitrarily selective individuals from the global memory, and h_1 has measured as:

$$h_1 = \alpha \times rand_1 \quad (10)$$

In which α indicates the constants, i.e., $\alpha \in [0,1]$, and $rand_1$ means the arbitrary value within [-1,1].

A novel individuals can be produced based on the subsequent equation for individuals in areas other than the region with bad-quality soils:

$$X_{inew} = h_2 \times (X_i - X_u) + X_i, (i = 1,2, \dots, n) \quad (11)$$

Whereas X_u represents the individual arbitrarily selective from every individual, and h_2 can be is measured as:

$$h_2 = \beta \times rand \quad (12)$$

In which β implies the constant, i.e., $\beta \in [0,1]$; and $rand$ represents the arbitrary number among 0 and 1. Every individual X_i can fuse with best individual in global or local memory by employing as:

$$X_{inew} = \begin{cases} X_i + \omega_1^d \times (X_i - G(B)), & Q > rand \\ X_i + rand \times (X_i - L(B)), & else \end{cases} \quad (13)$$

whereas $G(B)$ and $L(B)$ imply the best individual from global as well as local memory of every area correspondingly; Q means the constant, viz., $Q \in [0,1]$, and their value was generally 0.7 if no particular instruction was given; $rand$ denotes the arbitrary number among 0 and 1; and ω_1^d is $\omega 1$ at d^{th} iteration and diminishes with iteration method based on the subsequent equation:

$$\omega_1^{d+1} = \omega_1^d \times rand \quad (14)$$

whereas ω_1^1 is ω_1 refers custom integer, a primary iteration and generally equals 1 for achieving higher outcomes.

Doi: https://doi.org/10.54216/IJAACI.050103
Received: June 17, 2023 Revised: November 11, 2023 Accepted: December 19, 2023

Algorithm 1: Pseudocode of FFOA
$Input$: $N, D, U, L,$ Max FEs
Output: Minimal value in $f(X)$
Parameter initializin$(g\ N, D, U, L, k, n, \alpha, \beta, \omega_1, MaxFEs)$
Initializing population X with (4)
For dd to MaxFEs
Divide farmland regions with (5),
Detection of the worst area of soil with (6)
Upgrading memory with (7) and (8)
Optimized soil with (9), (10), (11), and (12)
Upgrading X and $f(X)$
Combined soil with (13)
Upgrading X and $f(X)$
Upgrading $\omega 1$ with (14)
End for

The FFOA manners grow a FF to reach greater classifier results and also determined the positive values for demonstrating the good outcome of candidate outcomes. In this paper, the minimalizing of classifier error rate is treated that FF.

$$fitness(x_i) = ClassifierErrorRate(x_i)$$
$$= \frac{No.of\ misclassified\ samples}{Total\ No.of\ samples} * 100 \quad (15)$$

D. Image Classification: Optimal CFNN Model

In this work, the CFNN model exploits the produced feature vectors and classifies them into the presence and absence of COVID19. CFNN is a kind of NN model that act in the same way as a feedforward neural network (FNN) [21]. The considerable variation between CFNN and FNN is that the relationship between the input and prior hidden layers has the benefit of incorporating the nonlinear connection without removing the linear connections between the input and the output. Furthermore, it is a mainstream network which needs less neurons to overcome the problem as compared to FNN making it effective and compact. By using the data from the input layer (I_i), a weighted sum is described by the summation function and a biased value (b_i), which is generally a constant number, is added to modify the output. The activation function (f_{act}) transmits this weighted amount into an output value. In the presented CFNN, the activation function applied for hidden and output layers are tangent sigmoid (a_1) and pure linear (a_2). The equation of (a_1) and (a_2) functions are represented as follows:

$$a_1 = \frac{1 - e^{-2x}}{1 + e^{-2x}} \quad (16)$$

$$a_2 = x \quad (17)$$

The calculation at output neuron $(0uT_k)$ and single hidden neuron (H_i) are demonstrated as follows:

$$H_i = f_{act}(\sum_{i=0}^{m}(I_i \times W_{ij}) + b_i) \quad (18)$$

Doi: https://doi.org/10.54216/IJAACI.050103
Received: June 17, 2023 Revised: November 11, 2023 Accepted: December 19, 2023

$$0uT_k = f_{act}(\sum_{k=0}^{n}(H_j \times W_{jk} + I_i \times W_{ik}) + b_k) \quad (19)$$

Let W_{ij}, W_{jk}, and W_{ik} be the vector of weights, H_j refers to the hidden neuron, and b_k indicates the biased value.

Lastly, the Adamax optimizer is utilized for the optimal tuning of the parameters linked to the CFNN model. Adamax is an optimizer system utilized in DL for updating network weights. It can be a variation of the Adam optimizer system and utilizes the infinity norm of gradients for scaling the rate of learning [22]. Adamax is established for performing like that huge databases and is frequently utilized to train DNNs. Adamax utilizes the infinity norm of gradients rather than the L2 norm utilized from the Adam technique. This permits greater upgrades in cases where the gradients can be sparse. It utilizes bias correction to account for primary higher momentum from the start of the trained procedure. It calculates an exponential weight moving average of gradient and squared gradient that can be utilized for measuring the 1st and 2nd moments of gradients.

4. Results and Discussion

The COVID-19 detection outcomes of the FFOADL-HDM method is studied using CT scans. Table 1 describes the details of the dataset.

Table 1: Details of dataset

Class	No. of Samples
Positive	1262
Negative	1230
Total No. of Samples	2492

Fig. 3 illustrates the confusion matrices of the FFOADL-HDM technique on the COVID19 classification system. The outcomes show the FFOADL-HDM technique has properly recognized the COVID19 positive and negative samples.

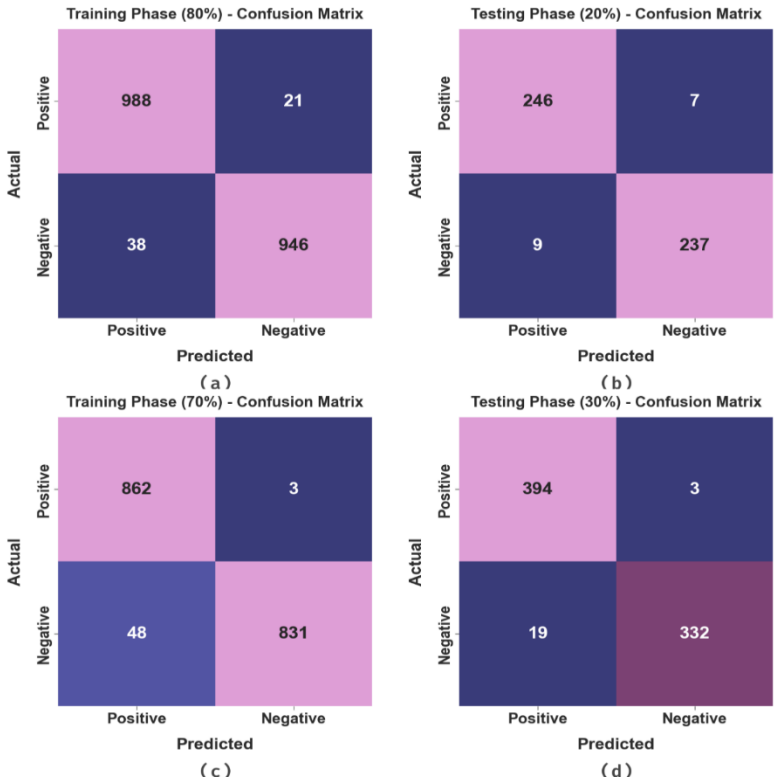

Figure 3: Confusion matrices of FFOADL-HDM method (a-b) TRP/TSP of 80:20 and (c-d) TRP/TSP of 70:30

Doi: https://doi.org/10.54216/IJAACI.050103
Received: June 17, 2023 Revised: November 11, 2023 Accepted: December 19, 2023

In Table 2, the COVID-19 classifier results of the FFOADL-HDM system are tested with 80:20 of TRP/TSP. Fig. 4 indicates the overall COVID19 classification performance of the FFOADL-HDM technique on 80% of TRP. The outcomes highlighted that the FFOADL-HDM technique has accurately classified the positive and negative COVID-19 samples. It is observed that the FFOADL-HDM method has detected the samples with average $accu_{bal}$ of 97.03%, $sens_y$ of 97.03%, $spec_y$ of 97.03%, F_{score} of 97.04%, and MCC of 94.09%.

Table 2: COVID-19 classifier outcomes of FFOADL-HDM method on TRP/TSP of 80:20

Class	$Accu_{bal}$	$Sens_y$	$Spec_y$	F_{score}	MCC
TRP (80%)					
Positive	97.92	97.92	96.14	97.10	94.09
Negative	96.14	96.14	97.92	96.98	94.09
Average	97.03	97.03	97.03	97.04	94.09
TSP (20%)					
Positive	97.23	97.23	96.34	96.85	93.59
Negative	96.34	96.34	97.23	96.73	93.59
Average	96.79	96.79	96.79	96.79	93.59

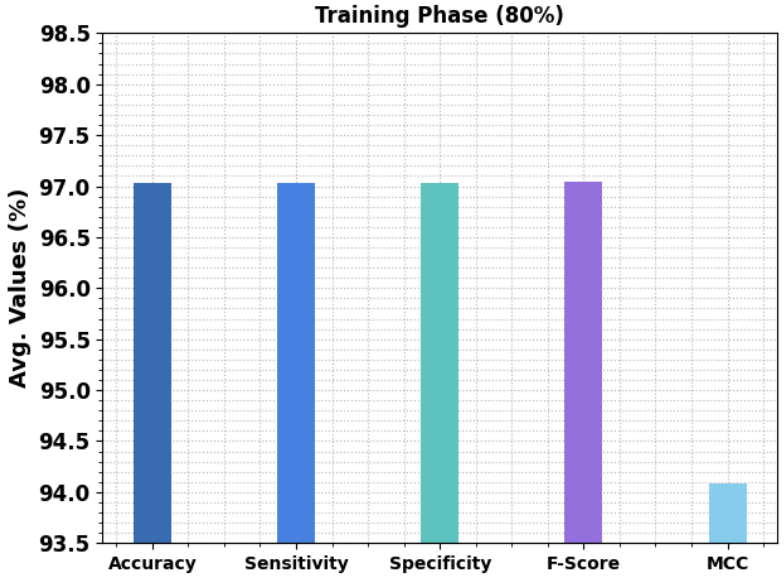

Figure 4: Average outcome of FFOADL-HDM approach on TRP of 80%

Fig. 5 specifies the overall COVID19 classification outcome of the FFOADL-HDM approach on 20% of TSP. The outcomes exhibited by the FFOADL-HDM approach have precisely classified the positive and negative COVID19 samples. It is noted that the FFOADL-HDM method has recognized the samples with an average $accu_{bal}$ of 96.79%, $sens_y$ of 96.79%, $spec_y$ of 96.79%, F_{score} of 96.79%, and MCC of 93.59%.

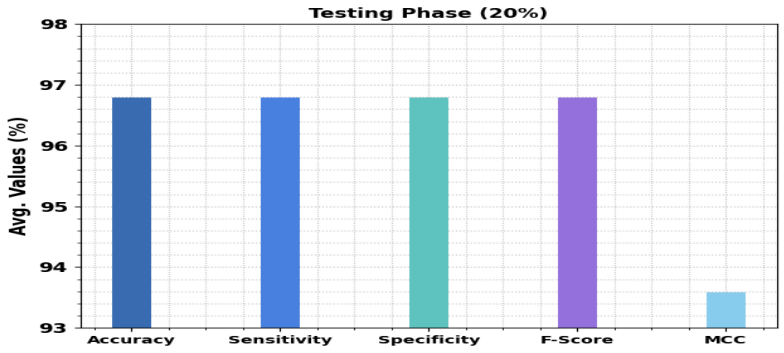

Figure 5: Average outcome of FFOADL-HDM method on TSP of 20%

Doi: https://doi.org/10.54216/IJAACI.050103
Received: June 17, 2023 Revised: November 11, 2023 Accepted: December 19, 2023

Table 3 provides a detailed comparison study of the FFOADL-HDM technique to assure the enhanced COVID19 detection results [23]. Fig. 6 reports a comparative analysis of the FFOADL-HDM technique with existing methods with respect to $sens_y$ and $spec_y$. The results show the improvements of the FFOADL-HDM method with increasing values of $sens_y$ and $spec_y$. Based on $sens_y$, the FFOADL-HDM technique reaches a higher $sens_y$ of 97.1% while the KELM, SVM, VGG16, ResNet152-V2, Inception-ResNet, and DenseNet models obtain lower $sens_y$ values of 95.97%, 96.06%, 95.23%, 96.35%, 92.06%, and 96.29% correspondingly.

Table 3: Comparative outcome of FFOADL-HDM technique with other existing methodologies

Methods	$Sens_y$	$Spec_y$	$accu_y$	F_{score}
FFOADL-HDM	97.1	97.1	97.10	97.07
KELM	95.97	96.23	95.39	95.24
SVM	96.06	96.69	95.76	95.54
VGG16	95.23	95.67	95.45	95.49
Resnet152-V2	96.35	92.43	94.91	95.09
Inception-ResNet	92.06	89.72	90.90	91.09
DenseNet	96.29	96.21	96.25	96.29

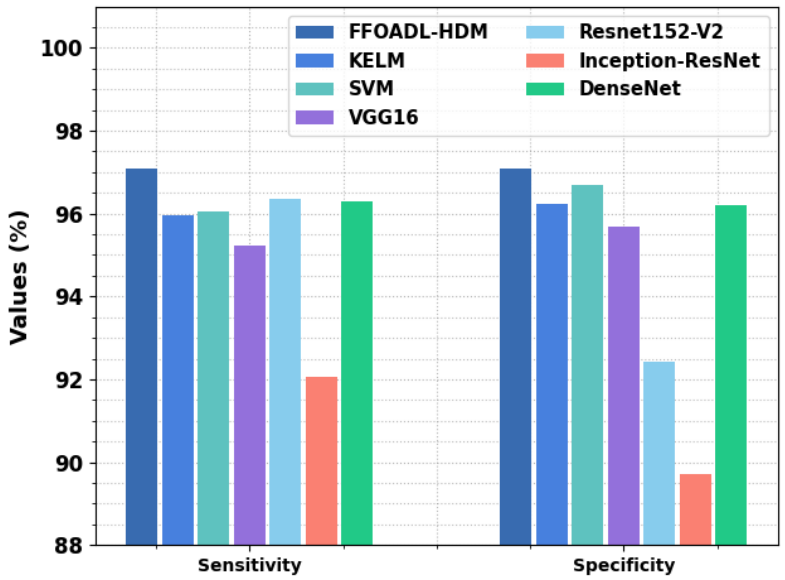

Figure 6: $Sens_y$ and $Spec_y$ outcome of FFOADL-HDM method with other existing techniques

In addition, based on $spec_y$, the FFOADL-HDM method reaches a higher $spec_y$ of 97.1% while the KELM, SVM, VGG16, ResNet152-V2, Inception-ResNet, and DenseNet approaches gain lower $spec_y$ values of 96.23%, 96.69%, 95.67%, 92.43%, 89.72%, and 96.21% correspondingly.

Fig. 7 reports a brief study of the FFOADL-HDM technique with existing approaches with respect to $accu_y$ and F_{score}. The outcomes revealed the improvements in the FFOADL-HDM technique with maximum values of $accu_y$ and F_{score}. Based on $accu_y$, the FFOADL-HDM approach reaches a higher $accu_y$ of 97.10% while the KELM, SVM, VGG16, ResNet152-V2, Inception-ResNet, and DenseNet methods gain lower $accu_y$ values of 95.39%, 95.76%, 95.45%, 94.91%, 90.90%, and 96.25% correspondingly.

Doi: https://doi.org/10.54216/IJAACI.050103
Received: June 17, 2023 Revised: November 11, 2023 Accepted: December 19, 2023

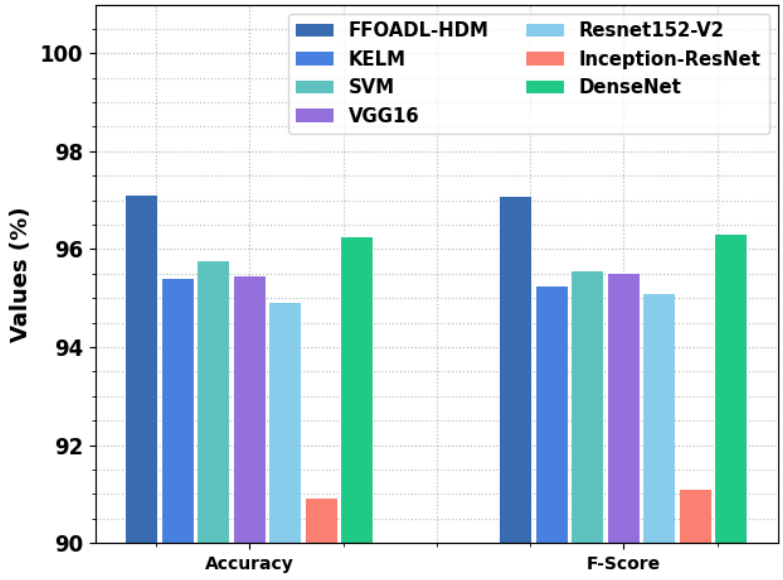

Figure 7: $Accu_y$ and F_{score} outcome of FFOADL-HDM method with other existing techniques

Also, based on F_{score}, the FFOADL-HDM technique reaches a higher F_{score} of 97.07% while the KELM, SVM, VGG16, ResNet152-V2, Inception-ResNet, and DenseNet approaches acquire lower F_{score} values of 95.24%, 95.54%, 95.49%, 95.09%, 91.09%, and 96.29% correspondingly. These outcomes confirmed the improved performance of the FFOADL-HDM method in the COVID-19 detection and classification process.

5. Conclusion

In this study, we have established a new FFOADL-HDM method for the COVID19 detection process. The proposed FFOADL-HDM technique mainly concentrated on the development of a COVID-19 classification technique utilizing CT scans. The proposed FFOADL-HDM method concentrated mainly on the development of the COVID-19 classification model using CT images. It encompasses a modified SqueezeNet feature extractor, FFOA-based hyperparameter tuning, CFNN-based classification, and Adamax optimizer-based parameter optimization. The FFOADL-HDM method makes use of a modified SqueezeNet model for the generation of feature vector. In addition, the hyperparameters of the modified SqueezeNet model can be selected by the use of FFOA. At last, the COVID-19 detection procedure can be executed by the use of an Adamax optimizer with the CFNN. The simulation analysis of the FFOADL-HDM approach is studied on the SARS-CoV-2 CT scan dataset from the Kaggle repository. The simulation values highlighted the enhanced detection rate of the FFOADL-HDM approach over recent state of art methods. In the future, hybrid DL algorithms can be designed to improve the detection rate of the FFOADL-HDM technique.

Funding: "This research received no external funding"

Conflicts of Interest: "The authors declare no conflict of interest."

References

[1] Che Azemin, M.Z., Hassan, R., Mohd Tamrin, M.I. and Md Ali, M.A., 2020. COVID-19 deep learning prediction model using publicly available radiologist-adjudicated chest X-ray images as training data: preliminary findings. International Journal of Biomedical Imaging, 2020.

[2] Khan, I.U., Aslam, N., Anwar, T., Alsaif, H.S., Chrouf, S.M.B., Alzahrani, N.A., Alamoudi, F.A., Kamaleldin, M.M.A. and Awary, K.B., 2022. Using a deep learning model to explore the impact of clinical data on covid-19 diagnosis using chest x-ray. Sensors, 22(2), p.669.

[3] Rasheed, J., Hameed, A.A., Djeddi, C., Jamil, A. and Al-Turjman, F., 2021. A machine learning-based framework for diagnosis of COVID-19 from chest X-ray images. Interdisciplinary Sciences: Computational Life Sciences, 13(1), pp.103-117.

[4] Zhang, J., Xie, Y., Li, Y., Shen, C. and Xia, Y., 2020. Covid-19 screening on chest x-ray images using deep learning based anomaly detection. arXiv preprint arXiv:2003.12338, 27.

Doi: https://doi.org/10.54216/IJAACI.050103
Received: June 17, 2023 Revised: November 11, 2023 Accepted: December 19, 2023

[5] Wang, G., Liu, X., Shen, J., Wang, C., Li, Z., Ye, L., Wu, X., Chen, T., Wang, K., Zhang, X. and Zhou, Z., 2021. A deep-learning pipeline for the diagnosis and discrimination of viral, non-viral and COVID-19 pneumonia from chest X-ray images. Nature biomedical engineering, 5(6), pp.509-521.
[6] Castiglioni, I., Ippolito, D., Interlenghi, M., Monti, C.B., Salvatore, C., Schiaffino, S., Polidori, A., Gandola, D., Messa, C. and Sardanelli, F., 2021. Machine learning applied on chest x-ray can aid in the diagnosis of COVID-19: a first experience from Lombardy, Italy. European radiology experimental, 5(1), pp.1-10.
[7] Yoo, S.H., Geng, H., Chiu, T.L., Yu, S.K., Cho, D.C., Heo, J., Choi, M.S., Choi, I.H., Cung Van, C., Nhung, N.V. and Min, B.J., 2020. Deep learning-based decision-tree classifier for COVID-19 diagnosis from chest X-ray imaging. Frontiers in medicine, 7, p.427.
[8] Zargari Khuzani, A., Heidari, M. and Shariati, S.A., 2021. COVID-Classifier: An automated machine learning model to assist in the diagnosis of COVID-19 infection in chest x-ray images. Scientific Reports, 11(1), pp.1-6.
[9] Wang, D., Mo, J., Zhou, G., Xu, L. and Liu, Y., 2020. An efficient mixture of deep and machine learning models for COVID-19 diagnosis in chest X-ray images. PloS one, 15(11), p.e0242535.
[10] Loey, M., El-Sappagh, S. and Mirjalili, S., 2022. Bayesian-based optimized deep learning model to detect COVID-19 patients using chest X-ray image data. Computers in Biology and Medicine, 142, p.105213.
[11] Hasoon, J.N., Fadel, A.H., Hameed, R.S., Mostafa, S.A., Khalaf, B.A., Mohammed, M.A. and Nedoma, J., 2021. COVID-19 anomaly detection and classification method based on supervised machine learning of chest X-ray images. Results in Physics, 31, p.105045.
[12] Shahin, O.R., Alshammari, H.H., Taloba, A.I. and Abd El-Aziz, R.M., 2022. Machine learning approach for autonomous detection and classification of COVID-19 virus. Computers and Electrical Engineering, 101, p.108055.
[13] Goyal, S. and Singh, R., 2021. Detection and classification of lung diseases for pneumonia and Covid-19 using machine and deep learning techniques. Journal of Ambient Intelligence and Humanized Computing, pp.1-21.
[14] Ismael, A.M. and Şengür, A., 2021. Deep learning approaches for COVID-19 detection based on chest X-ray images. Expert Systems with Applications, 164, p.114054.
[15] Ahemad, M.T., Hameed, M.A. and Vankdothu, R., 2022. COVID-19 detection and classification for machine learning methods using human genomic data. Measurement: Sensors, 24, p.100537.
[16] Hasan, Z. (2023). Deep Learning for Super Resolution and Applications. *Galoitica: Journal of Mathematical Structures and Applications*, 8(2), 34-42.
[17] Le, D.N., Parvathy, V.S., Gupta, D., Khanna, A., Rodrigues, J.J. and Shankar, K., 2021. IoT enabled depthwise separable convolution neural network with deep support vector machine for COVID-19 diagnosis and classification. International journal of machine learning and cybernetics, pp.1-14.
[18] https://www.kaggle.com/datasets/plameneduardo/sarscov2-ctscan-dataset
[19] Bernardo, L.S., Damaševičius, R., Ling, S.H., de Albuquerque, V.H.C. and Tavares, J.M.R., 2022. Modified SqueezeNet Architecture for Parkinson's Disease Detection Based on Keypress Data. Biomedicines, 10(11), p.2746.
[20] Sakthivel, S. and Prabhu, V., 2022. Optimal Deep Learning-Based Vocal Fold Disorder Detection and Classification Model on High-Speed Video Endoscopy. Journal of Healthcare Engineering, 2022.
[21] Alzayed, M., Chaoui, H. and Farajpour, Y., 2021. Maximum power tracking for a wind energy conversion system using cascade-forward neural networks. IEEE transactions on sustainable energy, 12(4), pp.2367-2377.
[22] Yi, D., Ahn, J. and Ji, S., 2020. An effective optimization method for machine learning based on ADAM. Applied Sciences, 10(3), p.1073.
[23] Jaiswal, A., Gianchandani, N., Singh, D., Kumar, V. and Kaur, M., 2021. Classification of the COVID-19 infected patients using DenseNet201 based deep transfer learning. Journal of Biomolecular Structure and Dynamics, 39(15), pp.5682-5689.

Doi: https://doi.org/10.54216/IJAACI.050103
Received: June 17, 2023 Revised: November 11, 2023 Accepted: December 19, 2023